2016.05.28 Journal Club

THE JOURNAL OF PHYSICAL CHEMISTRY C

Article

pubs.acs.org/JPCC

Second Harmonic and Sum-Frequency Generation from Aqueous Interfaces Is Modulated by Interference

Grazia Gonella,[†,#] Cornelis Lütgebaucks,[‡,#] Alex G. F. de Beer,[‡] and Sylvie Roke[*,‡]

[†]Max Planck Institute for Polymer Research, Ackermannweg 10, 55128 Mainz, Germany

[‡]Laboratory for fundamental BioPhotonics (LBP), Institute of Bioengineering (IBI), and Institute of Materials Science (IMX), School of Engineering (STI), and Lausanne Centre for Ultrafast Science (LACUS), École Polytechnique Fédérale de Lausanne (EPFL), CH-1015 Lausanne, Switzerland

Supporting Information

ABSTRACT: The interfacial region of aqueous systems also known as the electrical double layer can be characterized on the molecular level with second harmonic and sum-frequency generation (SHG/SFG). SHG and SFG are surface specific methods for isotropic liquids. Here, we model the SHG/SFG intensity in reflection, transmission, and scattering geometry taking into account the spatial variation of all fields. We show that, in the presence of a surface electrostatic field, interference effects, which originate from oriented water molecules on a length scale over which the potential decays, can strongly modify the probing depth as well as the expected intensity at ionic strengths $<10^{-3}$ M. For reflection experiments this interference phenomenon leads to a significant reduction of the SHG/SFG intensity. Transmission mode experiments from aqueous interfaces are hardly influenced. For SHG/SFG scattering experiments the same interference leads to an increase in intensity and to modified scattering patterns. The predicted scattering patterns are verified experimentally.

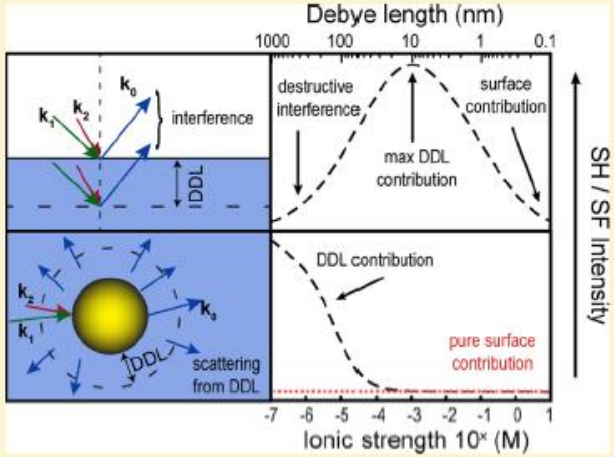

SH/SF generation at reflection geometry

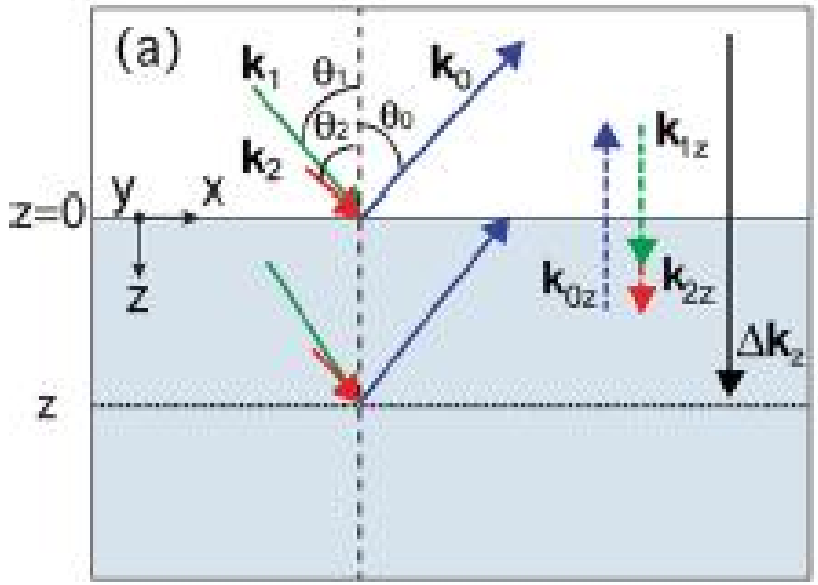

$n_{1,SFG} = n_{1,VIS} = n_{1,IR} = 1$

$n_{2,SFG} > n_{2,VIS} > n_{2,IR}$

$$\vec{E}(\omega_{SFG} = \omega_{IR} + \omega_{VIS}) \propto \chi^{(2)} : \vec{E}(\omega_{IR})\vec{E}(\omega_{VIS})$$

$$E_i(\omega_{SFG})e^{i\vec{k}_{SFG}\cdot\vec{r}} \propto \chi_{ijk}^{(2)} E_j(\omega_{IR})e^{i\vec{k}_{IR}\cdot\vec{r}} E_k(\omega_{VIS})e^{i\vec{k}_{VIS}\cdot\vec{r}}$$

SH/SF generation at reflection geometry

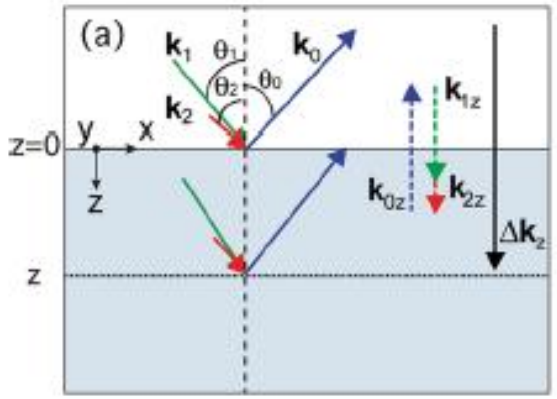

$$\Delta k_x = n_{2,VIS}\,|k_{VIS}|\,\sin\theta'_1 + n_{2,IR}\,|k_{IR}|\,\sin\theta'_2 - n_{2,SFG}\,|k_{SFG}|\sin\theta'_0$$
$$= n_{1,VIS}\,|k_{VIS}|\,\sin\theta_1 + n_{1,IR}\,|k_{IR}|\,\sin\theta_2 - n_{1,SFG}\,|k_{SFG}|\,\sin\theta_0$$

$$\Delta k_z = n_{2,VIS}\,|k_{VIS}|\,\cos\theta'_1 + n_{2,IR}\,|k_{IR}|\,\cos\theta'_2 + n_{2,SFG}\,|k_{SFG}|\cos\theta'_0$$

*Coherence length, l_c is given as,

$$l_{c,r} = \frac{1}{\Delta k_z} = \frac{1}{(n_{2,VIS}\,|k_{VIS}|\cos\theta_1' + n_{2,IR}\,|k_{IR}|\cos\theta_2' + n_{2,SF}\,|k_{SF}|\cos\theta_0')}$$

SH/SF generation at transmission geometry

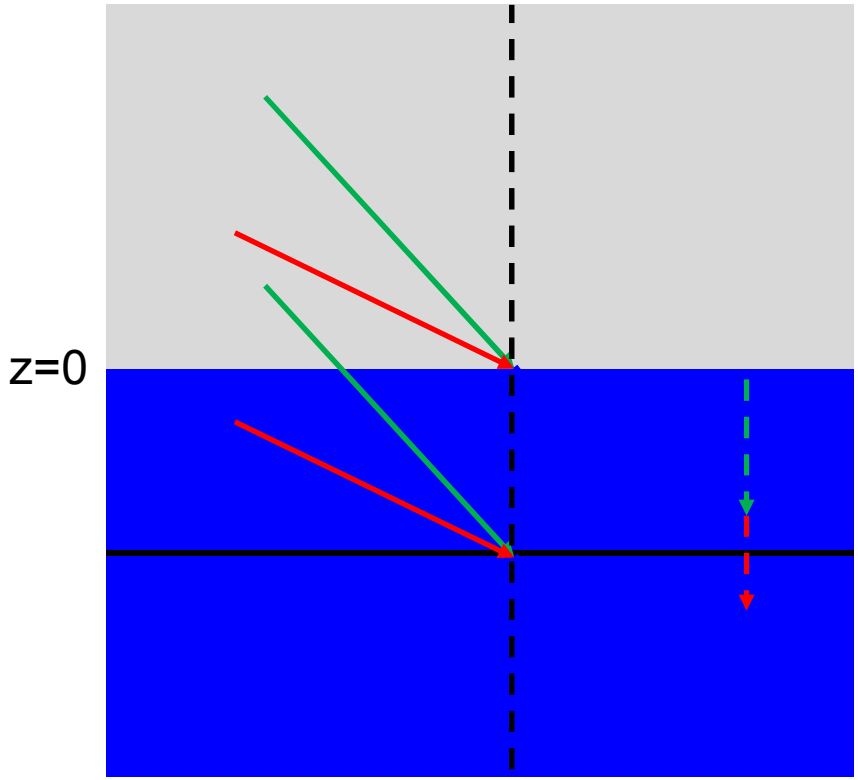

$$\Rightarrow l_{c,t} = \frac{1}{\Delta k_z} = \frac{1}{(n_{2,VIS}\left|k_{VIS}\right|\cos\theta_1^{'} + n_{2,IR}\left|k_{IR}\right|\cos\theta_2^{'} - n_{2,SF}\left|k_{SF}\right|\cos\theta_0^{'})} >> l_{c,r}$$

Calculation on our beam geometry

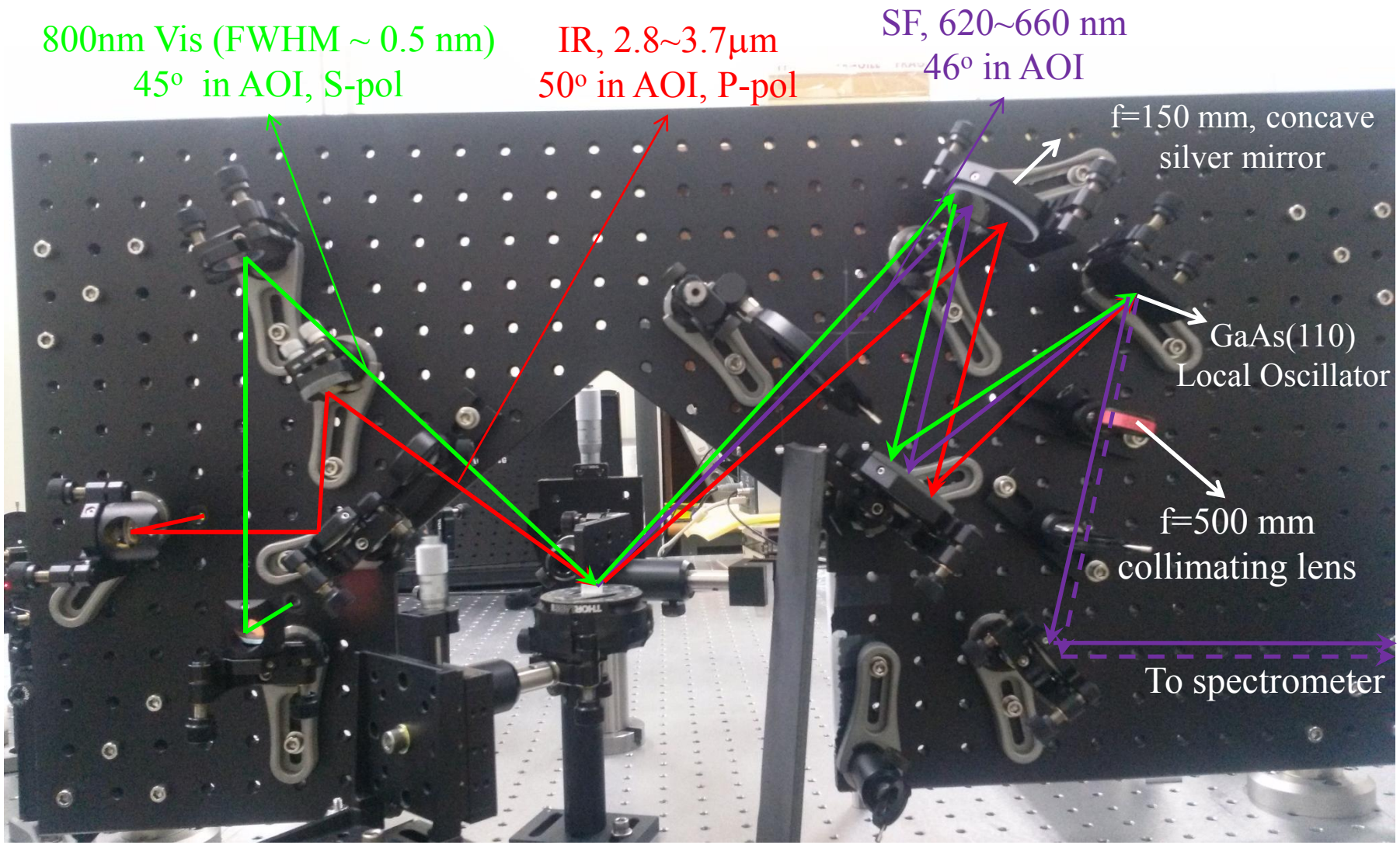

$l_{c,r} \sim 40$ nm $\qquad$ $l_{c,t} \sim 12\ \mu$m

Experimental Examples – OTS monolayer

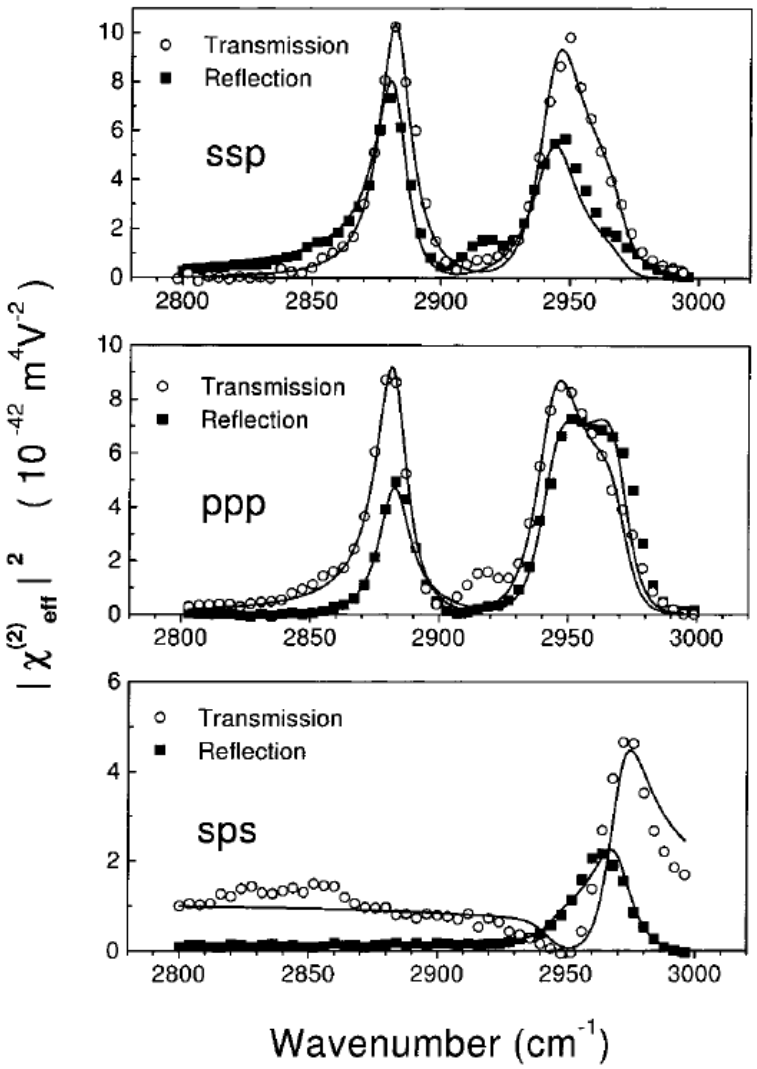

Figure 2. SFG spectra of an OTS monolayer on fused quartz. Points are experiment data, and the curves are theoretical fits.

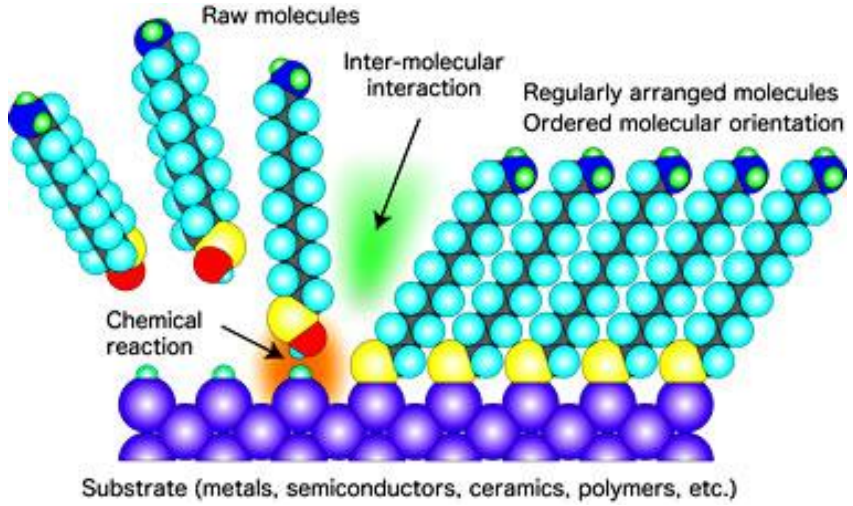

Thickness ~ 2 - 3 nm

Wei et al. J. Phys. Chem. B **2000,** *104,* 3349-3354.

Experimental Example – PE film

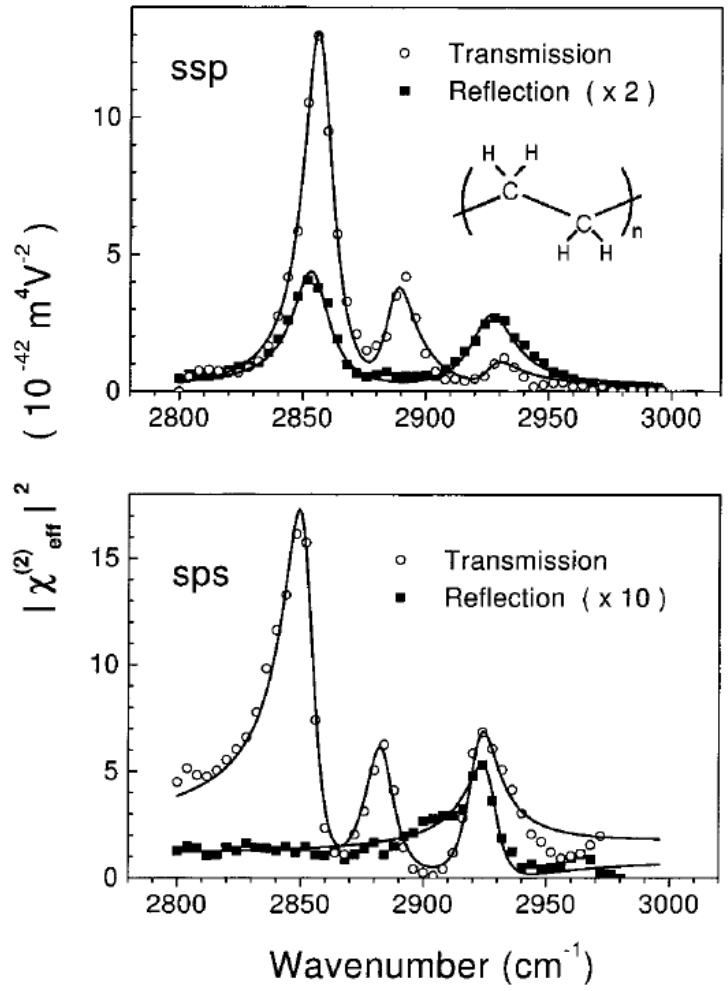

Figure 3. SFG spectra of a polyethylene film on fused quartz. The solid curves are theoretical fits.

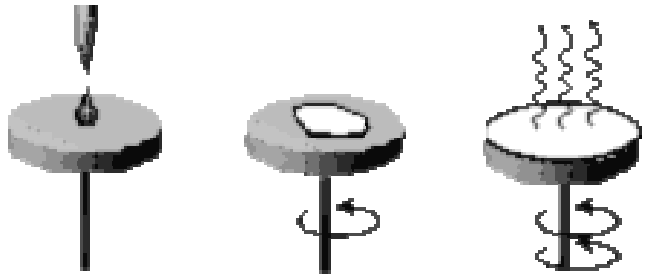

Thickness ~ 200 μm

Wei et al. J. Phys. Chem. B **2000,** *104,* 3349-3354.

Interfacial structure model: BIL and DL

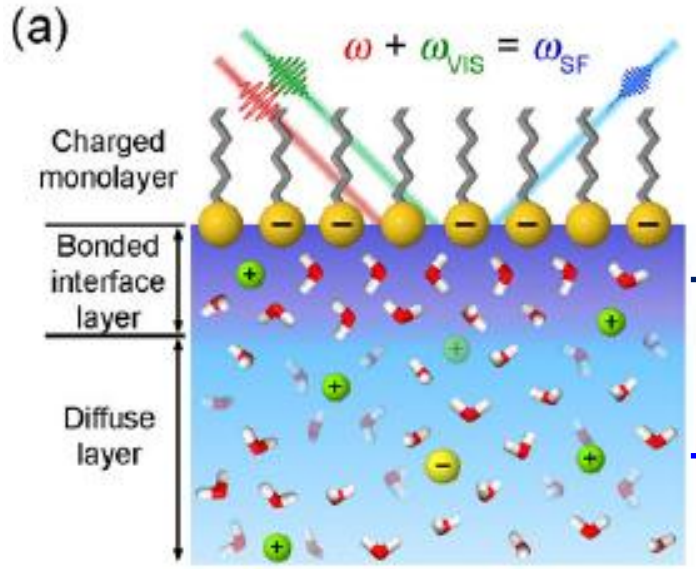

Water molecules strongly interacting with charged headgroups and counter cations.

Water molecules reoriented by surface electric field.

Wen et al. PRL **2016,** *116,* 016101.

$$\chi^{(2)}_{S,\text{eff}} = \chi^{(2)}_{S} + \int_{0^+}^{\infty} [\chi^{(2)}_{B} + \chi^{(3)}_{B} \cdot \hat{z} E_0(z')] e^{i\Delta k_z z'} dz' \qquad (1)$$

$\chi^{(2)}_S$: Second-order susceptibility of bonded interface layer

$\chi^{(2)}_B$: Second-order electric quadrupole bulk susceptibility

$\chi^{(3)}_B$: Third-order bulk susceptibility

Δk_z : Phase mismatch in reflection geometry ($\Delta k_z = k_{SF,z} - k_{Vis,z} - k_{IR,z}$)

Surface potential profile depending on salt concentration

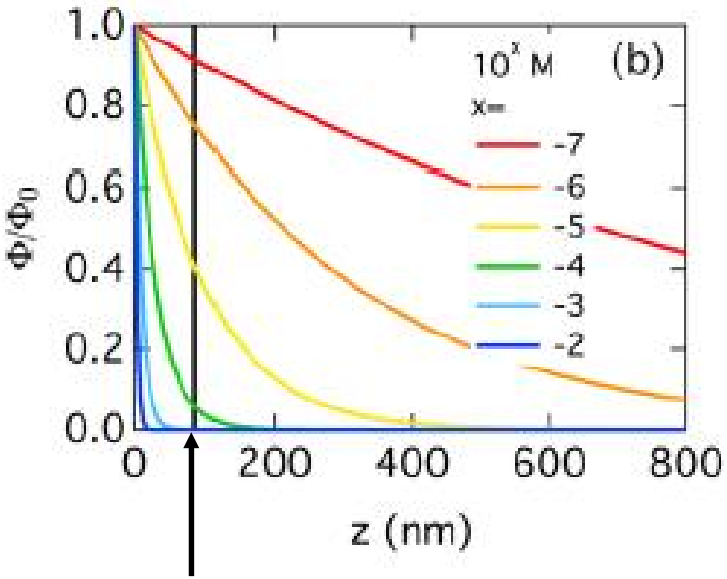

$$l_{c,r} \sim 90 \text{ nm}$$

Surface SHG (800nm excitation, AOI 45°)

< Gouy-Chapman model >

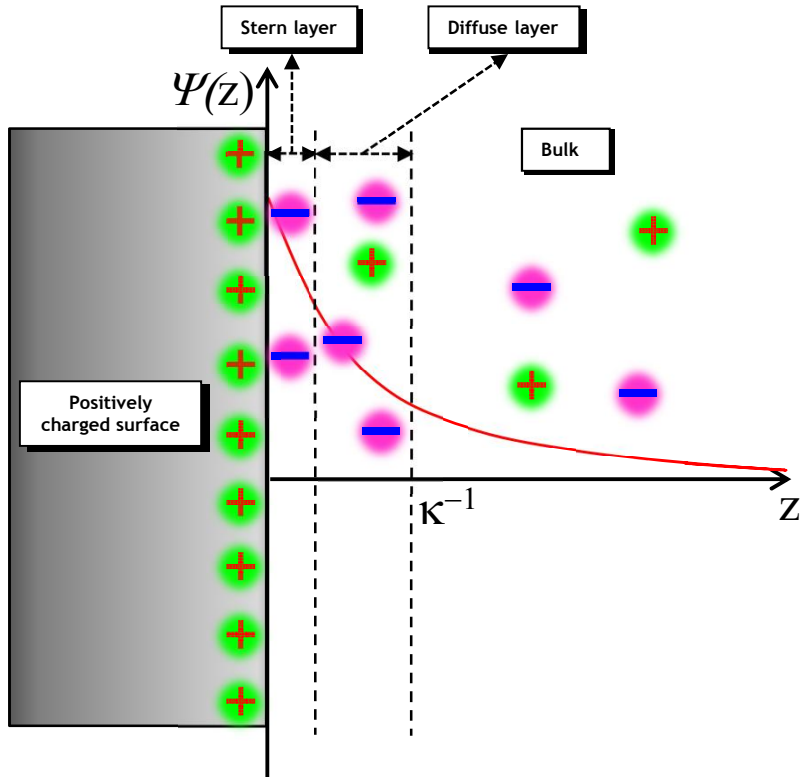

$$\mathbf{P}^{(2)}(\omega_0) = \varepsilon_0 \boldsymbol{\chi}_s^{(2)} : \mathbf{E}_1(\omega_1)\mathbf{E}_2(\omega_2)$$

$$P^{(3)}(\omega_0) = \varepsilon_0 \int_0^{+\infty} \chi^{(3)'} E_1(\omega_1, k_1) E_2(\omega_2, k_2) E_{DC}(z) e^{i\Delta k_z z} \, dz$$

Considering phase mismatching correction

$$P^{(3)}(\omega_0) = \varepsilon_0 \int_0^{+\infty} \chi^{(3)'} E_1(\omega_1, k_1) E_2(\omega_2, k_2) E_{DC}(z) e^{i\Delta k_z z} \, dz$$

$$P^{(3)}(\omega_0) = \varepsilon_0 \chi^{(3)'} E_1(\omega_1) E_2(\omega_2) \int_0^{+\infty} \left(-\frac{d}{dz}\Phi(z)\right) e^{i\Delta k_z z} \, dz$$

$$P^{(3)}(\omega_0) = \varepsilon_0 \chi^{(3)'} E_1(\omega_1) E_2(\omega_2) (\Phi_0 + i\Delta k_z \int_0^{+\infty} \Phi(z) e^{i\Delta k_z z} \, dz)$$

Calculation result

$$I(\omega_0) \propto I_1(\omega_1) I_2(\omega_2) \left| \chi_s^{(2)} + \chi^{(3)'} \Phi_0 \frac{\kappa}{\kappa - i\Delta k_z} \right|^2$$

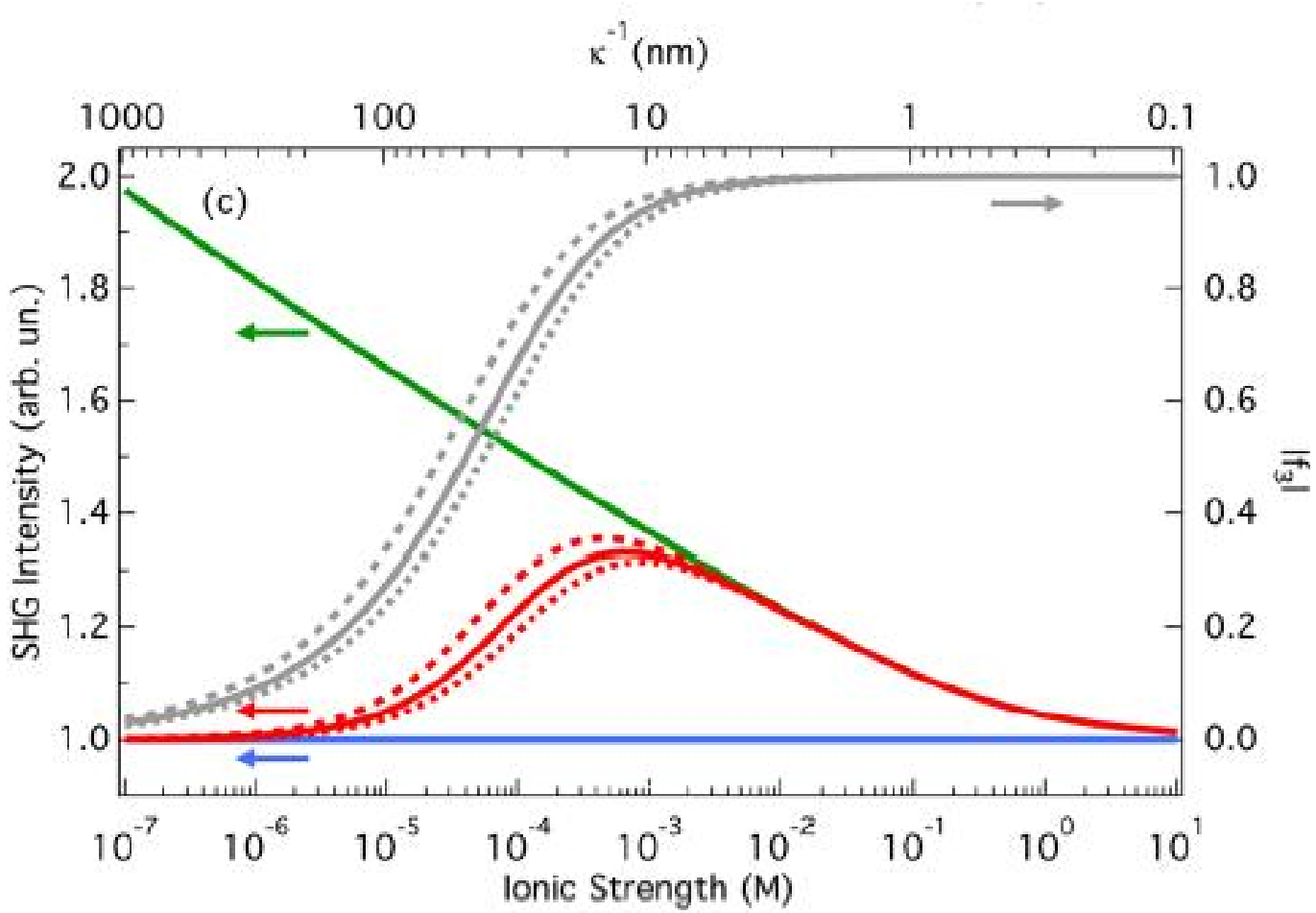

Transmission and scattering geometry

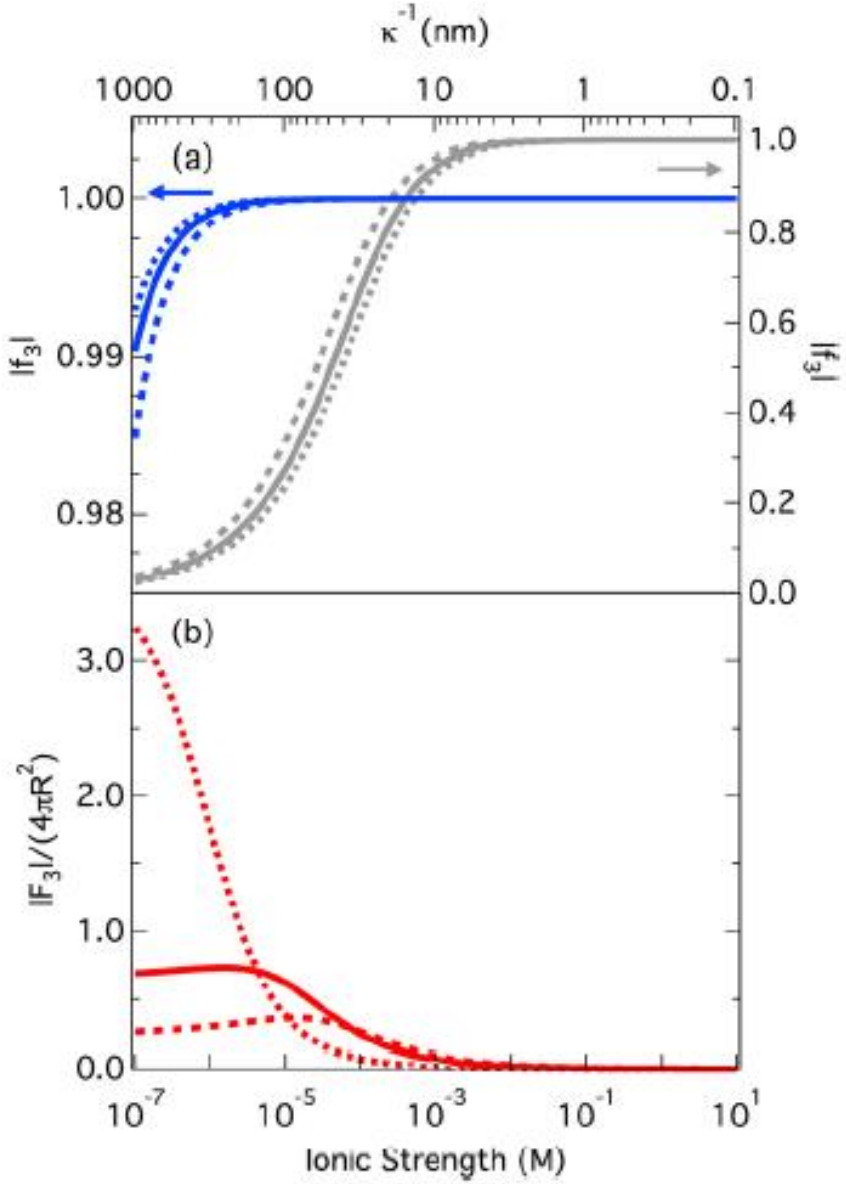

Figure 2. (a) $|f_3(\kappa, \Delta k_z)|$ in transmission geometry (blue continuous curve, left axis) and reflection geometry (gray continuous curve, right axis), as a function of ionic strength. We used the following input values: $\theta_1 = \theta_2 = 45°$, $\lambda_1 = \lambda_2 = 800$ nm, $n_{air} = 1$, $n_{H_2O}(800\text{ nm}) = 1.33$, and $n_{H_2O}(400\text{ nm}) = 1.34$. The dotted (dashed) line corresponds to curves calculated for $\theta_1 = \theta_2 = 10°$ ($\theta_1 = \theta_2 = 80°$). (b) $|F_3(\kappa R, qR)|/(4\pi R^2)$ for a scattering geometry calculated as a function of ionic strength c. We used the following as parameters: $\theta = 45°$, $\lambda_1 = \lambda_2 = 1028$ nm, $n_{air} = 1$, $n_{H_2O}(1028\text{ nm}) = 1.33$, and $n_{H_2O}(514\text{ nm}) = 1.33$, and $R = 50$ nm. The continuous, dotted, and dashed lines correspond to curves calculated at scattering angles $\theta = 45°$, 10°, and 80°, respectively.

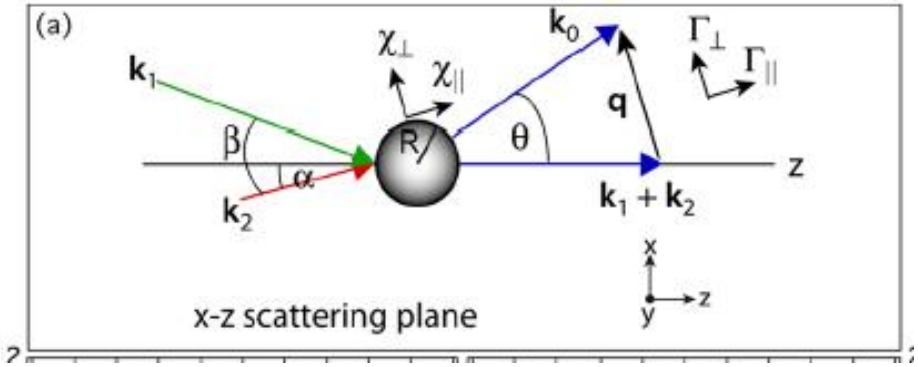

SFG/SHG scattering

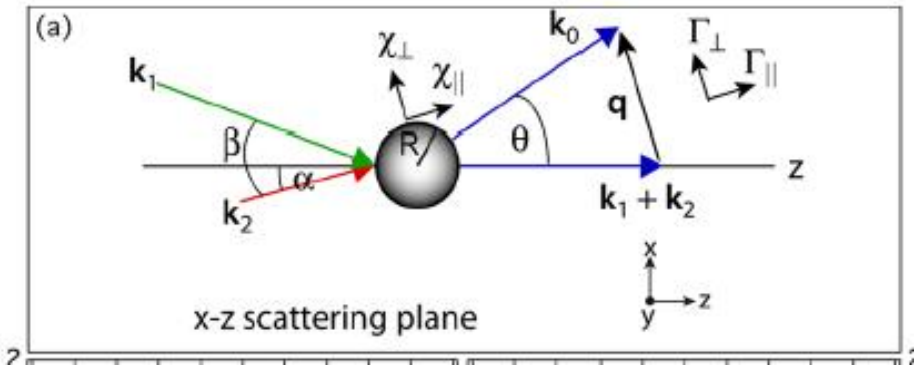

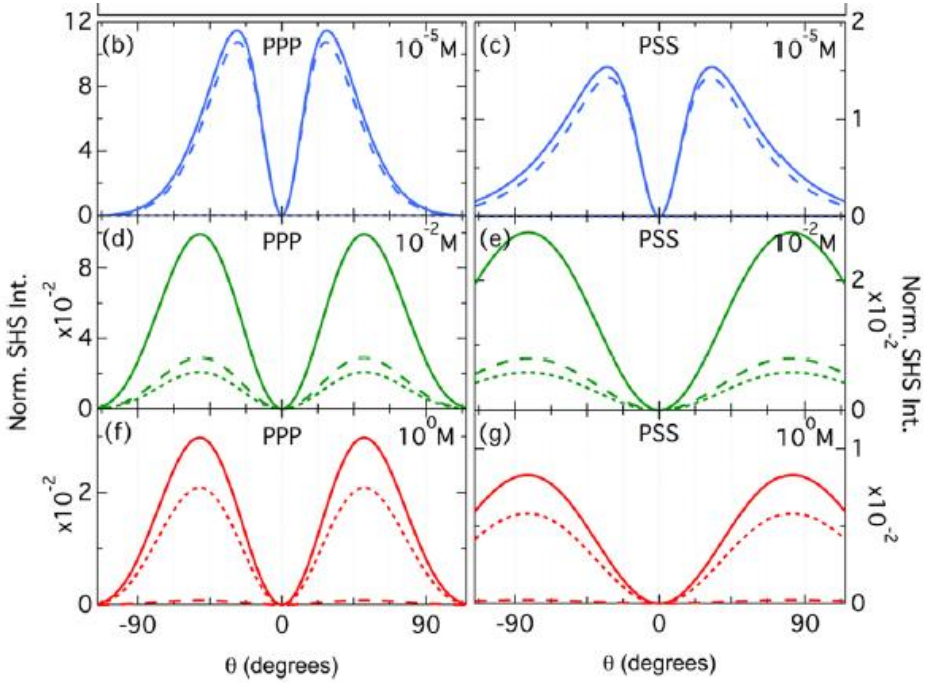

$$\Gamma_n^{(3)'} = -\int_R^{+\infty} \frac{\mathrm{d}\Phi(r)}{\mathrm{d}r}\Gamma_n^{(3)}(r)\,\mathrm{d}r$$

$$= 2F_1(qR)\Phi_0\chi_n^{(3)'} + 2\chi_n^{(3)'}\int_R^{+\infty}\frac{\mathrm{d}F_1(qr)}{\mathrm{d}r}\Phi(r)\,\mathrm{d}r \qquad \Phi(r) = \Phi_0\frac{R}{r}\mathrm{e}^{-\kappa(r-R)}$$

$$\Gamma_n^{(3)'} = 2\Phi_0\chi_n^{(3)'}(F_1(qR) + F_3(\kappa R, qR)) \qquad F_3(\kappa R, qR) = 2\pi R^2 \mathrm{i}\frac{qR\cos(qR) + \kappa R\sin(qR)}{(qR)^2 + (\kappa R)^2}$$

SHG scattering measurement

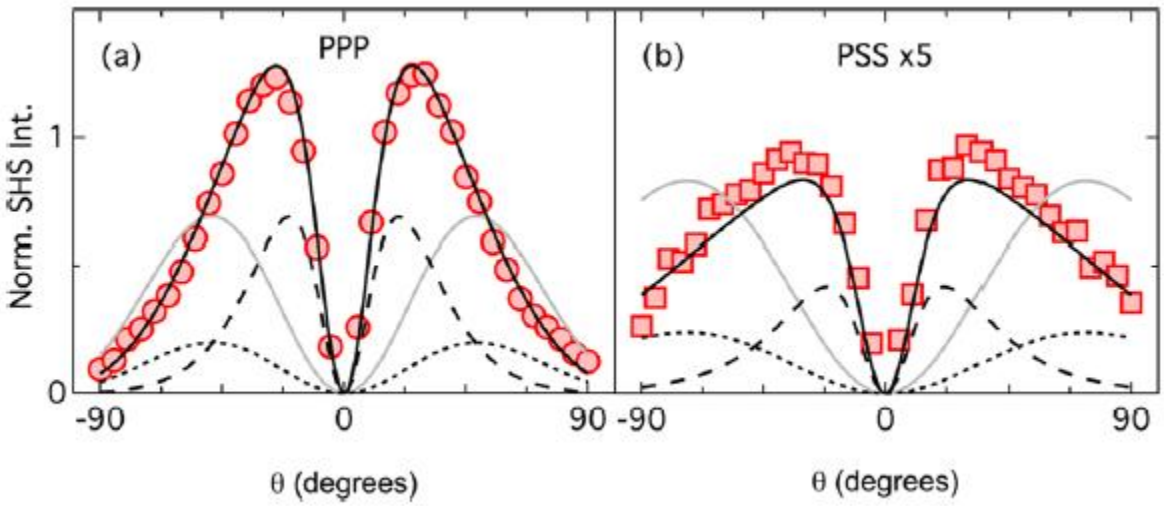

Figure 4. SHS intensity patterns of hexanol-covered hexadecane droplets in ultrapure water for (a) PPP and (b) PSS polarization combinations. The best fit (black line) was achieved using eq 17 for $\mathbf{\Gamma}^{(3)\prime}$, i.e., using the contribution of $F_3(\kappa R, qR)$ to describe the behavior at low ionic strength. The gray line represents the best fit without the $F_3(\kappa R, qR)$ correction, i.e., using eq 15 for $\mathbf{\Gamma}^{(3)\prime}$. The intensities originating from a pure surface response, $\chi^{(3)\prime} = 0$, and pure bulk response, $\chi_s^{(2)} = 0$, are displayed as dotted and dashed lines, respectively.

Zeta potential measurement :
-37 mV of surface potential